

Robustness of Variational Quantum Algorithms against stochastic parameter perturbation

Daniil Rabinovich,^{1,2} Ernesto Campos,¹ Soumik Adhikary,¹
Ekaterina Pankovets,^{1,2} Dmitry Vinichenko,^{1,3} and Jacob Biamonte⁴

¹*Skolkovo Institute of Science and Technology, Moscow, Russian Federation*

²*Moscow Institute of Physics and Technology, Moscow, Russian Federation*

³*Moscow Engineering Physics Institute, Moscow, Russian Federation*

⁴*Beijing Institute of Mathematical Sciences and Applications, Beijing, China*

Variational quantum algorithms are tailored to perform within the constraints of current quantum devices, yet they are limited by performance-degrading errors. In this study, we consider a noise model that reflects realistic gate errors inherent to variational quantum algorithms. We investigate the decoherence of a variationally prepared quantum state due to this noise model, which causes a deviation from the energy estimation in the variational approach. By performing a perturbative analysis of optimized circuits, we determine the noise threshold at which the criteria set by the stability lemma is met. We assess our findings against the variational quantum eigensolver and quantum approximate optimization algorithm for various problems with up to 14 qubits. Moreover, we show that certain gate errors have a significantly smaller impact on the coherence of the state, allowing us to reduce the execution time without compromising performance.

I. INTRODUCTION

Noisy Intermediate Scale Quantum (NISQ) computing [1] is constrained by limited coherence times and operation precision [2–5], which restrict the number of qubits and circuit depths that can be implemented with reasonable fidelity. This limits the range of possible experimental demonstrations. The variational model of quantum computation is tailored to operate within these practical limitations [6–8], and has been shown to be computationally universal under idealized conditions [9]. Similar to machine learning, a variational algorithm employs a parameterized quantum circuit, called an ansatz, that is iteratively adjusted to minimize a cost function in a quantum-to-classical feedback loop [10]. The cost function usually takes the form of the expectation of a problem Hamiltonian, where the ground state of the problem Hamiltonian represents the solution to a given problem instance. By minimizing the cost function (energy), a variational algorithm aims to approximate the ground state of the Hamiltonian. However, this approach does not guarantee the quality of the approximate solution, which is typically measured by the overlap between the state prepared by the ansatz and the true ground state. Nonetheless, the overlap can be bounded. Using the stability lemma [9], it has been demonstrated that the bounds can be directly linked to the energy, allowing us to determine the energy threshold (upper bound) required to ensure a minimum (fixed) overlap. We refer to this as the acceptance threshold, and a state with an energy below this threshold is considered accepted by the algorithm.

Variational algorithms are designed to mitigate some of the systematic limitations of NISQ devices [8, 11–13]. However, these algorithms are still susceptible to stochastic noise. While there is some evidence that variational algorithms can benefit from a certain level of stochas-

tic noise [14], in general, noise negatively impacts their performance by inducing decoherence and degrading solution quality.

In this paper, we investigate how errors in the form of parameter deviations impact the performance of variational algorithms when operated at their noiseless optimal parameters. We analytically demonstrate that the energy shift varies quadratically with the spread of parameter deviation, equivalent to an energy shift linear with respect to the gate error probabilities for various noise models [15]. We validate our findings introducing the noise to the Variational Quantum Eigensolver (VQE) employed for Ising Hamiltonian, and the Quantum Approximate Optimization Algorithm (QAOA) for 3-SAT [16], MAX-CUT [17] and unstructured search [18, 19]. Furthermore, we observe the performance to be more resilient to alterations in certain parameters. Based on these findings, we propose methods to potentially enhance performance and reduce the execution time of variational quantum algorithms.

II. PRELIMINARIES

A. Variational Quantum Eigensolver

VQE is a variational algorithm designed to approximate the ground state and energy of a given n -qubit problem Hamiltonian H . The approximation to the ground state is prepared using a tunable quantum circuit (a.k.a. ansatz) $U(\boldsymbol{\theta})$ as $|\psi(\boldsymbol{\theta})\rangle = U(\boldsymbol{\theta})|0\rangle^{\otimes n} = \left(\prod_k U_k(\theta_k)\right)|0\rangle^{\otimes n}$ with tunable parameters $\theta_k \in [0, 2\pi)$. Upon the preparation of quantum state $|\psi(\boldsymbol{\theta})\rangle$, local measurements are used to calculate the energy $E(\boldsymbol{\theta}) = \langle\psi(\boldsymbol{\theta})|H|\psi(\boldsymbol{\theta})\rangle$. Finally, a classical co-processor iteratively tunes variational parameters to minimize the en-

ergy function, to identify

$$\boldsymbol{\theta}^* \in \arg \min_{\boldsymbol{\theta}} E(\boldsymbol{\theta}), \quad (1)$$

$$E^* = \min_{\boldsymbol{\theta}} E(\boldsymbol{\theta}), \quad (2)$$

which gives an approximation to the ground energy of H .

A certain type of VQE, called Quantum Approximate Optimization Algorithm (QAOA) [17] was specifically designed to approximately solve combinatorial optimization problems [16, 17, 20–30]. In this algorithm the combinatorial problem is encoded into a diagonal problem Hamiltonian H , whose ground state encodes the solution to the original problem. The algorithm makes use of a problem-dependent ansatz of depth p , which prepares a variational state $|\psi_p(\boldsymbol{\gamma}, \boldsymbol{\beta})\rangle$ as

$$|\psi_p(\boldsymbol{\gamma}, \boldsymbol{\beta})\rangle = \prod_{k=1}^p e^{-i\beta_k H_x} e^{-i\gamma_k H} |+\rangle^{\otimes n}, \quad (3)$$

with real parameters $\gamma_k \in [0, 2\pi)$, $\beta_k \in [0, \pi)$. Here $H_x = \sum_{j=1}^n X_j$ is the standard one-body mixer Hamiltonian with Pauli matrix X_j applied to the j -th qubit. Similar to standard VQE, the algorithm minimizes the energy cost function $E(\boldsymbol{\gamma}, \boldsymbol{\beta}) = \langle \psi_p(\boldsymbol{\gamma}, \boldsymbol{\beta}) | H | \psi_p(\boldsymbol{\gamma}, \boldsymbol{\beta}) \rangle$ as in (1) and (2) with $\boldsymbol{\theta} = (\boldsymbol{\gamma}, \boldsymbol{\beta})$. The state $|\psi_p(\boldsymbol{\gamma}^*, \boldsymbol{\beta}^*)\rangle$ approximates the ground state of H and hence encodes the solution to the original problem. Nevertheless, in any VQE the quality of the approximation, quantified as the overlap between the true solution and the approximate solution, is not known a priori from (1). Still, one can establish bounds on this quantity using the so called stability lemma.

B. Stability lemma

The stability lemma states that if $|g\rangle$ is the true ground state of H with energy E_g and Δ is the spectral gap (the difference between the ground state energy and the energy of the first excited state) the following relation holds [9, 31]:

$$1 - \frac{E^* - E_g}{\Delta} \leq |\langle \psi_p(\boldsymbol{\gamma}^*, \boldsymbol{\beta}^*) | g \rangle|^2 \leq 1 - \frac{E^* - E_g}{E_m - E_g} \quad (4)$$

where E_m is the maximum eigenvalue of H . Thus to guarantee a non-trivial overlap one must ensure that $E^* \leq E_g + \Delta$. We call the latter the acceptance condition.

III. QUANTUM CIRCUITS IN THE PRESENCE OF REALISTIC GATE ERRORS

Implementation of unitary operations used in variational ansatz depends significantly on the considered hardware. Typically the implementation makes use of

electromagnetic pulses, such as in superconducting quantum computers [32, 33], neutral atom based quantum computers [34, 35], and trapped ion based quantum computers [8, 36]. Such pulses can change the population of the energy levels that constitute a qubit or introduce phases to the quantum amplitudes, thus controlling the state of the qubits. Fluctuations in the pulse shape, phase and amplitude will affect the operation and reduce its fidelity [37, 38]. As in typical unitary operations the angles of rotations depend on time averaged intensity $I(t)$ of the electromagnetic pulse ($\theta \propto \int I(t) dt$), variations in pulse parameters can result in stochastic deviations of the angles from the desired values, which becomes increasingly important for fast gate realizations [39]. Moreover, these angle deviations can be present even in the case of perfectly stabilized pulses: in ion based quantum computers thermal motion reduces certainty in ions positions, leading to variations in the ion-laser couplings [37, 40] and causing deviations in the resulting angles [39]. This type of error can contribute gate infidelity of about $10^{-3} - 10^{-2}$ [40, 41]; while other sources of noise would also contribute to gate imperfections, the discussed model becomes the dominant source of error for certain setups, such as ground state ion qubits with radial modes [42].

In such settings if a quantum circuit is composed of the parameterised gates $\{U_k(\theta_k)\}_{k=1}^q$; $\theta_k \in [0, 2\pi)$ and one tries to prepare a state $|\psi(\boldsymbol{\theta})\rangle = \prod_{k=1}^q U_k(\theta_k) |\psi_0\rangle$, a different state

$$|\psi(\boldsymbol{\theta} + \boldsymbol{\delta\theta})\rangle = \prod_{k=1}^q U(\theta_k + \delta\theta_k) |\psi_0\rangle, \quad (5)$$

is prepared instead due to the presence of errors. Notice here that the perturbation $\boldsymbol{\delta\theta}$ to the parameters is stochastic and is sampled with a certain probability density $p(\boldsymbol{\delta\theta})$. This implies that the prepared state can be described by an ensemble $\{|\psi(\boldsymbol{\theta} + \boldsymbol{\delta\theta})\rangle, p(\boldsymbol{\delta\theta})\}$, which can be treated as a density matrix

$$\rho(\boldsymbol{\theta}) = \int_{\boldsymbol{\delta\theta} \in [-\pi, \pi]^q} p(\boldsymbol{\delta\theta}) |\psi(\boldsymbol{\theta} + \boldsymbol{\delta\theta})\rangle \langle \psi(\boldsymbol{\theta} + \boldsymbol{\delta\theta})| d(\boldsymbol{\delta\theta}). \quad (6)$$

Eq. (6) represents a noise model native to the variational paradigm of quantum computing. Thus, for the rest of the paper we systematically study the effect of this noise model on the performance of Variational Quantum Algorithms, specifically VQE and QAOA. In particular we study the energy perturbation around E^* in different scenarios subsequently recovering the strength of noise under which the acceptance condition continues to be satisfied.

IV. ENERGY OF PERTURBED QUANTUM CIRCUITS

In this section we present our analytical and numerical findings on the robustness of VQE against the noise model discussed in Section III. Specifically, we study how energy $E = \langle \psi(\boldsymbol{\theta}) | H | \psi(\boldsymbol{\theta}) \rangle$ of a prepared variational state $|\psi(\boldsymbol{\theta})\rangle$ changes when $\boldsymbol{\theta}$ is perturbed. In our analysis we do not require $\boldsymbol{\theta}$ to be an optimum of the energy function, as in (1). Nevertheless, following the settings of VQE, we apply our analysis to optimized circuits $U(\boldsymbol{\theta}^*)$, which prepare the best possible approximations to the ground state for a given circuit depth. Finally, we substantiate our findings with numerical simulations of the perturbed optimized circuits.

A. Perturbative analysis in presence of gate errors

Consider a problem Hamiltonian H and a variational ansatz $|\psi(\boldsymbol{\theta})\rangle = U_1(\theta_1) \dots U_q(\theta_q) |\psi_0\rangle$ used to mini-

mize H . Here the gates $U_k(\theta_k)$ have the form:

$$U_k(\theta_k) = e^{iA_k\theta_k}, A_k^2 = \mathbb{1}. \quad (7)$$

A typical example of such an ansatz is the checkerboard ansatz [43], with Mølmer-Sørensen (MS) gates as the entangling two qubit gates. Nevertheless, any quantum circuit can admit a decomposition in terms of operations of the form (7); this adds generality to this assumption.

In the presence of gate errors the prepared quantum state decoheres as $|\psi(\boldsymbol{\theta})\rangle \rightarrow \rho(\boldsymbol{\theta})$ as per (6). To obtain the analytic form of $\rho(\boldsymbol{\theta})$ we first note that

$$U_k(\theta_k + \delta\theta_k) = U_k(\theta_k)U_k(\delta\theta_k) = \cos \delta\theta_k U_k(\theta_k) + \sin \delta\theta_k U_k\left(\theta_k + \frac{\pi}{2}\right).$$

This follows directly from (7). Therefore we get:

$$|\psi(\boldsymbol{\theta} + \boldsymbol{\delta\theta})\rangle\langle\psi(\boldsymbol{\theta} + \boldsymbol{\delta\theta})| = \sum_{k_1, \dots, k_q, m_1, \dots, m_q=0}^1 (\cos^2 \delta\theta_1 \tan^{k_1+m_1} \delta\theta_1) \dots (\cos^2 \delta\theta_q \tan^{k_q+m_q} \delta\theta_q) |\psi_{k_1 \dots k_q}\rangle\langle\psi_{m_1 \dots m_q}|, \quad (8)$$

where

$$|\psi_{k_1 \dots k_q}(\boldsymbol{\theta})\rangle = U_1\left(\theta_1 + k_1 \frac{\pi}{2}\right) \dots U_q\left(\theta_q + k_q \frac{\pi}{2}\right) |\psi_0\rangle. \quad (9)$$

Here we make three realistic assumptions—(a) perturbations to all the angles are independent, (b) the distribution is symmetric around zero, $p(\boldsymbol{\delta\theta}) = p(-\boldsymbol{\delta\theta})$ and (c) the distribution $p(\delta\theta_k)$ vanishes quickly outside the range $(-\sigma_k, \sigma_k)$; that is, the error is localized on the scale $\sigma_k \ll 1$. Note that if assumption (b) does not hold, as long as mean value $\langle \delta\theta_k \rangle$ is independent from the angle θ_k , one can always shift the parameters as $\theta_k \rightarrow \theta_k - \langle \delta\theta_k \rangle$ to avoid non-zero mean. Otherwise, terms linear in $\langle \delta\theta_k \rangle$ could contribute to the energy perturbation [44]. Notice that we do not require $\delta\theta_k$ to be small compared to the value θ_k .

Substituting (8) in (6) we arrive at the expression:

$$\rho(\boldsymbol{\theta}) = |\psi(\boldsymbol{\theta})\rangle\langle\psi(\boldsymbol{\theta})| + \delta\rho, \quad (10)$$

where

$$\delta\rho \approx - \sum_{k=1}^q a_k |\psi(\boldsymbol{\theta})\rangle\langle\psi(\boldsymbol{\theta})| + \sum_{k=1}^q a_k |\psi_k\rangle\langle\psi_k| + o(\sigma_k^2). \quad (11)$$

Here $|\psi_k\rangle \equiv |\psi_k(\boldsymbol{\theta})\rangle = |\psi_{00\dots 01\dots 00}(\boldsymbol{\theta})\rangle$ with 1 placed in the k -th position. We point out that the terms of the form $|\psi_k\rangle\langle\psi_m|$ for $k \neq m$ do not enter (11) as the associated factor $\langle \delta\theta_k \delta\theta_m \rangle = \langle \delta\theta_k \rangle \langle \delta\theta_m \rangle = 0$. Finally,

$$a_k \equiv \langle \sin^2 \delta\theta_k \rangle \approx \langle \delta\theta_k^2 \rangle = \int (\delta\theta_k)^2 p(\delta\theta_k) d(\delta\theta_k) \sim \sigma_k^2. \quad (12)$$

The numerical prefactor in the last transition depends on the exact form of the distribution and we neglect it for generality.

Notice that (11) can be viewed as the action of certain noisy channel, where each of the gates is altered with probability $a_k \sim \sigma_k^2$. In this sense, we call a_k gate error probabilities, though this treatment is specific to the interpretation of the noisy channel.

For the simplest case of identical distributions ($\sigma_k^2 = \sigma^2 = a$), the noise induced energy perturbation around

the noiseless value $E = \langle \psi(\boldsymbol{\theta}) | H | \psi(\boldsymbol{\theta}) \rangle$ becomes

$$\begin{aligned} \delta E &\equiv \text{Tr}(\rho(\boldsymbol{\theta})H) - E = \text{Tr}(\delta\rho H) \\ &\approx a \sum_{k=1}^q (\langle \psi_k | H | \psi_k \rangle - E), \end{aligned} \quad (13)$$

which demonstrates that energy perturbation depends linearly on the gate error probabilities a (quadratic in σ). A similar dependence on the gate error probabilities as observed earlier [15], albeit with a different noise model.

In the most general setting one cannot estimate energies $\langle \psi_k | H | \psi_k \rangle$, as they strongly depend on the problem Hamiltonian, considered ansatz and its parameters. Nevertheless, by imposing a trivial bound $\langle \psi_k | H | \psi_k \rangle \leq E_m$ we can establish

$$\delta E \leq qa(E_m - E) \sim q\sigma^2(E_m - E). \quad (14)$$

Now we turn to practical applications of VQE, where the ansatz attempts to approximate the ground state of the problem Hamiltonian. Following the optimization (1), noiseless energy E becomes E^* —the energy of the optimized circuit, which in the presence of noise increases by δE according to (14). According to the stability lemma (4), we request that noisy energy $E^* + \delta E < E_g + \Delta$ and conclude that for

$$\sigma < \sqrt{\frac{\Delta - (E^* - E_g)}{q(E_m - E^*)}} \quad (15)$$

the acceptance condition is still satisfied. In other words, this level of noise can be tolerated by the algorithm, as it still can produce states with certain overlap with the ground state. Obviously, this requires the original noiseless circuit to prepare a good approximation of the ground state, i.e. $E^* < E_g + \Delta$. In practice, however, the bound (15) can be significantly relaxed with tighter bounds on $\langle \psi_k | H | \psi_k \rangle$, possible only for specific problems.

When performing the approximation in (13) we disregarded higher powers of σ_k . In the most general case this is justified when $qa \sim q\sigma^2 \ll 1$, which can further be improved for specific problems, where terms like $\langle \psi_k | H | \psi_k \rangle$ could be estimated.

B. Numerical simulations of stochastic perturbations

While our perturbative analysis holds for all VQEs, we substantiate our findings by numerically minimizing instances of Ising Hamiltonian with checkerboard ansatz and implementing QAOA for a range of problems. Importantly, we numerically confirm validity of the quadratic approximation (13) all the way up to $q\sigma^2 \gtrsim 1$ for specific problems, significantly expanding applicability range of treatment compared to analytical predictions. Indeed, for realistic infidelities of NISQ devices ($a \sim 0.001 - 0.01$) this could allow for execution of thousands of gates.

In our numerical simulations we start by minimizing (finding the best approximation for the considered depth) specific problem Hamiltonians with chosen ansatz to identify optimal set of angles $\boldsymbol{\theta}^*$ ($(\boldsymbol{\gamma}^*, \boldsymbol{\beta}^*)$ for QAOA). Then the optimal circuit is subjected to the noise model described by (6); for that we randomly sample perturbations δ to each of the gate angles from a uniform distribution on the interval $(-\sigma, \sigma)$ and average the obtained energies.

1. VQE for Ising Hamiltonian

We begin by considering minimization of Ising Hamiltonian

$$H = \sum_{j=1}^n Z_j Z_{j+1} + h \sum_{j=1}^n X_j, \quad (16)$$

with the checkerboard ansatz, composed of Molmer-Sorensen (R_{XX}) [45, 46] entangling gates and local rotations. Here we set $Z_1 = Z_{n+1}$. We consider $n = 6, 8, 10$ with circuit depth $p = 8, 10, 12$ respectively, which, after optimization, guaranteed more than 50% overlap with the ground state. For every n we considered 100 instances of Hamiltonian (16) with transverse field in the range $h \in [0.8, 1.2]$. Subjecting every circuit to the discussed noise model, we average the energy perturbation over considered instances and obtain Fig. 1.

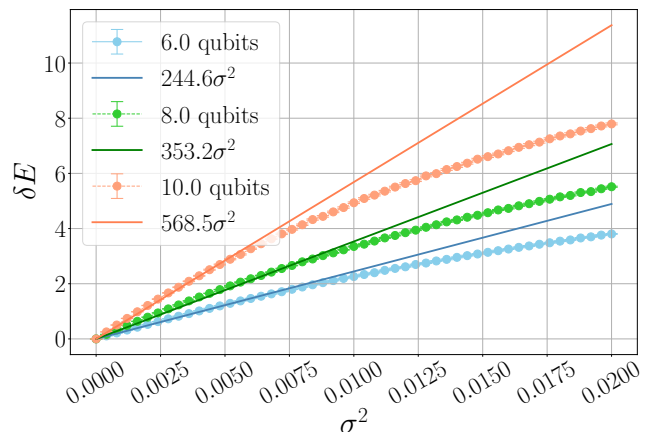


FIG. 1. Average energy increase of perturbed optimal VQE circuit of $n = 6, 8, 10$ qubits for circuit depth $p = 8, 10, 12$, obtained by the perturbation of $\boldsymbol{\theta}^*$ by δ uniformly sampled from the range $(-\sigma, \sigma)$. Error bars depict standard errors. Polynomial fits of data points confirm that $\delta E \propto \sigma^2$.

Indeed, it confirms our analytical prediction of quadratic scaling of δE with respect to σ up to $\sigma^2 \sim 10^{-2}$. Moreover, it can be seen that proportionality coefficient indeed is roughly proportional to number of gates in checkerboard ansatz $q = 5np$, as expected from (14). Importantly, the linear dependence prevails for σ up to $q\sigma^2 \gtrsim 1$ ($q = 240, 400, 600$ for $n = 6, 8, 10$ respectively), significantly expanding applicability of our result.

2. QAOA

In this section we focus on the effect of perturbing QAOA circuits, optimized to solve instances of various problems. We begin by considering 3-SAT problem, defined in appendix A. Importantly, in our numerical implementation the problem Hamiltonian propagator $e^{-i\gamma H}$ is realized as a sequence of gates of the type (7) (notice that H is naturally written in the Pauli basis, which gives the desired decomposition) to adhere to practical realizations. Angles in all these gates receive uncorrelated perturbations; the same holds for the single qubit gates implementing $e^{-i\beta H_x}$.

We ran QAOA for 100 uniformly generated 3-SAT instances of 6, 8, and 10 variables with 26, 34 and 42 clauses (corresponding to computational phase transition density of 4.2 for 3-SAT) and circuits of 15, 25 and 30 layers, respectively. All the instances were generated to have a unique satisfying assignment. The optimal circuits are then perturbed and the calculated energies are averaged over considered instances. The results are presented in Fig. 2. Again, it is seen that for small values of noise the energy scales as $\delta E \propto \sigma^2$, as per (14), which is equivalent to linear dependence on the gate error probabilities a_k . The linear behaviour is now limited to a smaller range of σ , compared to the case depicted in Fig. 1. This is caused by a larger gate count in the QAOA circuits (primarily from the decomposition of $e^{-i\gamma H}$): number of gates, averaged over the instances, reach $q = 555, 1525, 2610$ for $n = 6, 8, 10$ respectively. Nevertheless, the linear approximation remains valid up to $q\sigma^2 \gtrsim 5$, again improving over analytical predictions.

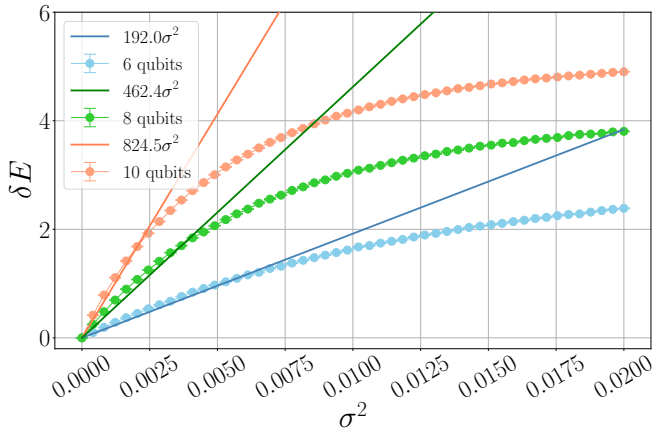


FIG. 2. Average energy shift of 100 uniformly generated 3-SAT instances of 6, 8 and 10 qubits obtained from perturbed optimal circuits of depth 15, 25 and 30, respectively. All instances were designed to have clause to variable ratio of 4.2 and a unique satisfying assignment. Error bars depict standard errors. Polynomial fits of data indicate $\delta E \propto \sigma^2$ up to $q\sigma^2 \gtrsim 5$.

These large gate counts q , induced by the circuit depth sufficient to solve 3-SAT, might already be beyond the

capabilities of current NISQ devices. However, if one were interested in a decent approximate solution to the considered problem, the required circuit depth could be reduced, allowing to meet NISQ realities. Indeed, we obtained decent approximate solutions to instances of 3-SAT with a fixed circuit depth $p = 10$, which constituted less than 1000 gates for up to $n = 10$ qubits, reaching at most 1500 gates for $n = 14$ qubits. By perturbing these circuit, we see that energy increase, depicted in Fig. 3, is better approximated by a linear dependence with respect to gate errors, compared to Fig. 2.

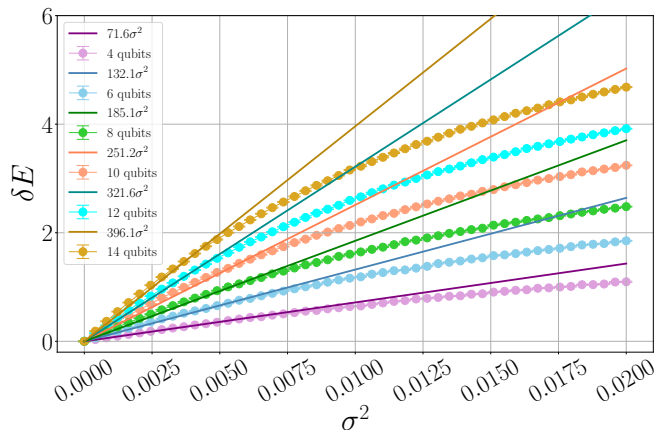


FIG. 3. Average energy shift of 100 uniformly generated 3-SAT instances of 6, 8 and 10 qubits obtained from perturbed optimal circuits of depth 10. All instances were designed to have clause to variable ratio of 4.2 and a unique satisfying assignment. Error bars depict standard errors. Polynomial fits of data indicate $\delta E \propto \sigma^2$ up to $q\sigma^2 \gtrsim 5$.

Additionally, in Appendix B we present results for QAOA solving instances of MAX-CUT and unstructured search (defined in Appendix A). Importantly, for the latter we considered the case of highly correlated perturbations (without decomposition of $e^{-i\gamma H}$ into gates of the form (7)) to demonstrate generalizability of our results. Both cases qualitatively agree with results obtained for VQE and MAX-SAT. Overall, based on the presented evidence we conclude that linear scaling of energy perturbation with respect to σ^2 prevails all the way up to $q\sigma^2 \gtrsim 1$. Thus, for the infidelities of current devices ($\sigma^2 \lesssim 0.001 - 0.01$) our prediction remains valid for circuits composed of thousands of gates. Importantly, actual values of energies deviate towards lower values, thus making our prediction a valid upper bound on energy perturbations even for larger number of gates and noise levels.

C. Perturbation to individual parameters

In this section we aim at comparing sensitivity of energy to perturbations of specific layers of QAOA circuits. For that we perturb the angles γ_k and β_k in (3) one at

a time by a constant δ , while the rest are kept intact. Effect of this perturbations on the energy is illustrated in Figures 4 and 5 for $n = 10$ qubits, while similar results were also obtained for $n = 6, 8$ qubits. These results are numerical and are yet to be explained analytically. We observe that perturbations to certain angles have a significantly smaller effect on the energy. Thus we can infer that reducing the values of such angles would not have a significant effect on performance. This would allow to reduce the circuit execution time t_{exec} in the implementations where it can be attributed to QAOA angles $t_{exec} \propto \sum_{k=1}^p \beta_k + \gamma_k$. Depending on the physical realisation, decrease of this sum can alternatively be attributed to a change in the amplitude of the applied pulse.

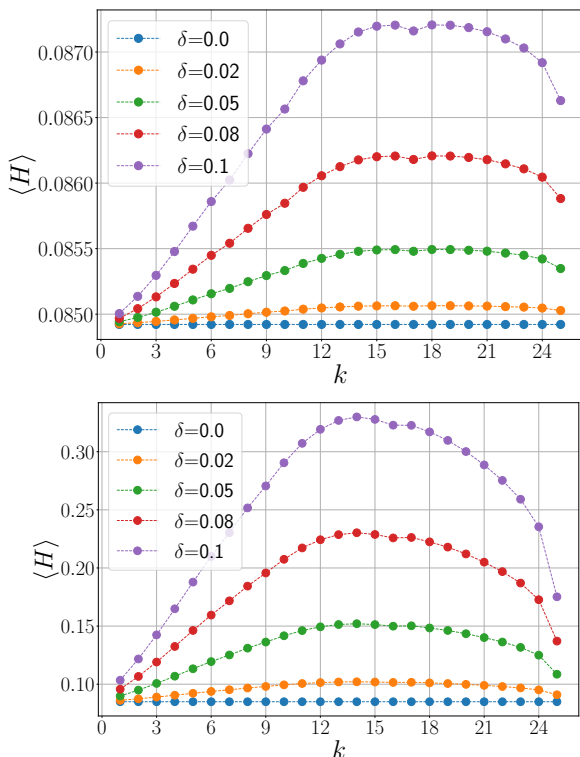


FIG. 4. Energy $\langle H \rangle = \langle \psi(\theta^* + \delta\theta) | H | \psi(\theta^* + \delta\theta) \rangle$ obtained for unstructured search with $n = 10$, $p = 25$, when only β_k (top) or γ_k (bottom) are perturbed by δ .

Reducing the execution time is important to quantum algorithms, since variational parameters are proportional to the time required to execute the gates experimentally. NISQ era devices suffer from limited coherence, thus reducing execution times can lead to more efficient hardware utilization [47, 48]. We test these ideas in the setting of unstructured search, as depicted in Fig. 6. Here we demonstrate QAOA energies for 6 qubits, optimized with an additional condition $t_{exec} \equiv \sum_{k=1}^p \beta_k + \gamma_k \leq t_{max}$ for multiple values of t_{max} and circuit depth p . This becomes a constrained optimization problem when $t_{max} < 3\pi p$ (see ranges for γ_k and β_k). The highlighted green and orange rectangles correspond to the two groups of opti-

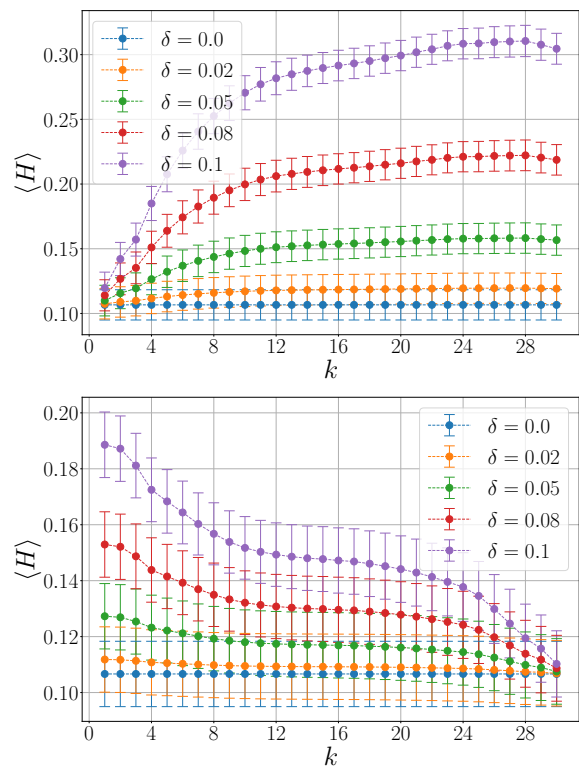


FIG. 5. Average energy $\langle H \rangle = \langle \psi(\theta^* + \delta\theta) | H | \psi(\theta^* + \delta\theta) \rangle$ of 100 uniformly generated 3-SAT instances solved with $p = 30$ layers, where β_k (top) or γ_k (bottom), from the k -th layer, are perturbed by δ . The instances are of $n = 10$ qubits with a clause to variable ratio of 4.2 and a unique satisfying assignment.

mal angles, obtained in the unconstrained optimization, that minimize the energy at each depth [18].

Several interesting conclusions could be drawn from Fig. 6. Firstly, it is evident that, for a fixed p , starting from a low value of t_{max} and progressively increasing it improves the performance only until the first set of optimal parameters is found (green rectangles). Past this point performance stagnates; nevertheless, for a sufficiently large value of t_{max} the other solution appears (orange rectangles). Thus, for a fixed depth, t_{exec} corresponding to orange boxes is always larger compared to that of the green boxes. Secondly, one may adopt several strategies for reducing execution time without compromising the performance. We illustrate this with a few examples.

Let us consider the labeled rectangles in Fig. 6. It is seen that for rectangle 1 $t_{exec} \approx 31$ is greater than that of rectangle 2 which has $t_{exec} \approx 25$. Thus by constraining t_{max} to values below 31, one can force optimization to find solution 2 instead of solution 1, keeping p fixed. This significantly reduces the execution time while maintaining a constant energy. Furthermore, keeping $t_{max} \approx 31$, one can increase the circuit depth from 6 to 7, thus going from rectangle 1 to 3. In doing so we achieve an improved energy. Note that although $t_{max} \approx 31$ for rectangle 3, the

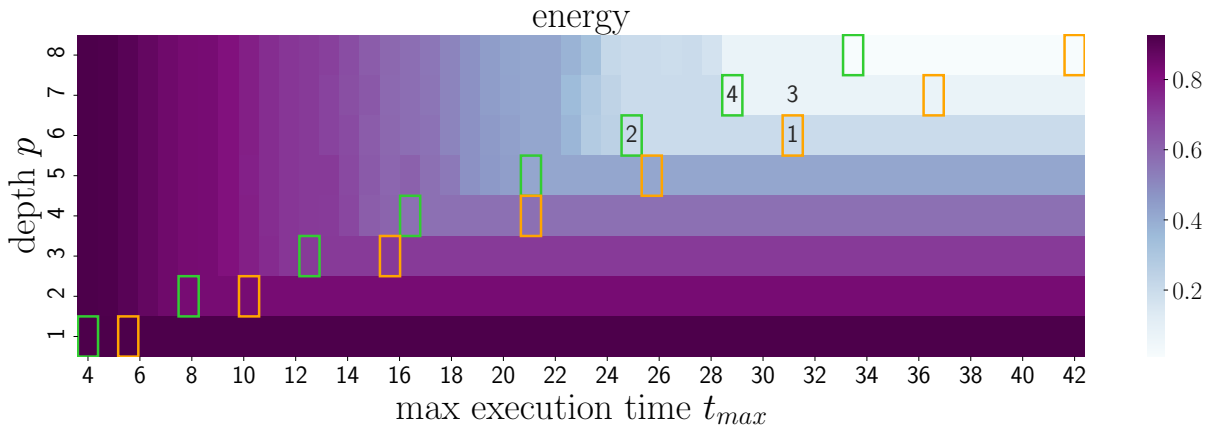


FIG. 6. Each cell in the figure represents the optimized energy for a given depth and a fixed maximal execution time. The coloring scheme is indicated on the right. Green and orange rectangles depict the two branches of angles that minimize expectation value for a given depth.

corresponding $t_{exec} \approx 29$ (same as the execution time of rectangle 4). Thus by including an extra layer we not only manage to improve the performance, but also reduce the execution time.

In general, for an arbitrary problem Hamiltonian one can not be sure if optimization has returned the ideal set of angles (green ones in our example). For this reason, one might employ several strategies based on the behaviour depicted in Fig. 6 to achieve a minimum threshold energy. These include—to reduce t_{max} until energy starts degrading or to increase depth with fixed t_{max} until performance stagnates.

V. DISCUSSION

In this study, we considered a noise model which naturally arises from the control laser pulse intensity fluctuation and spatial inhomogeneity and can become a dominant source of error for certain experimental setups. Within this model the gate parameters receive stochastic perturbation, which leads to an increase of the energy E^* of an optimized variational circuit. Through a perturbative analysis, we found that the change in energy δE due to the presence of the gate errors behaves quadratically with respect to the spread of parameter deviations, which is equivalent to linear dependence on the gate error probabilities. Using this result, we derived an upper bound on the level of noise that can be tolerated, satisfying the acceptance condition.

Our analytical findings are substantiated by numerical simulations of VQE for Ising chain with transversed field and QAOA for three common problems - 3-SAT, MAX-CUT and unstructured search - using different modifications of the considered noise model. We confirm that energy perturbation scales quadratically with σ^2 up to $q\sigma^2 \gtrsim 1$, expanding applicability of our result compared to analytical expectations. We study a wide range of

problem sizes and circuit depths, and show that for realistic values of $\sigma^2 \sim 10^{-3} - 10^{-2}$ the predicted behaviour prevails for circuits up to thousands of gates. Additionally, our numerical results showed that the algorithmic performance is more resilient to perturbations of certain variational parameters. Based on this observation, we proposed a strategy to improve performance and reduce the execution time of variational quantum algorithms. Specifically, we showed that the performance of QAOA is not affected when limiting the maximum execution time to $t_{max} = t_{exec} - \epsilon$ for $\epsilon \ll t_{exec}$. We also demonstrated that in some cases reducing t_{max} can lead to significant reductions in t_{exec} , while increasing the depth of the algorithm can lead to an energy reduction with fixed t_{exec} .

While we presented results for additive perturbation $\theta \rightarrow \theta + \delta\theta$, a multiplicative perturbation $\theta \rightarrow (1 + \epsilon)\theta$ might represent another realistic scenario. Nevertheless, qualitative behaviour for both types of errors was observed to be the same, therefore we focused on the additive scenario in the text. Importantly, whereas our study primarily focused on energy perturbations around the noiseless optimum θ^* , in practice, one has to train the algorithm in the presence of noise, which can change the optimal angles θ^* to $\theta^* + \delta\theta^*$, where the shift $\delta\theta^*$ depends on the strength of the noise. However, using perturbation theory around the noiseless optimum, one can estimate $\delta\theta^* = O(\sigma^2)$ in the regime of small noise, and the corresponding change in the energy is $\text{Tr}(\rho(\theta^* + \delta\theta^*)H) - \text{Tr}(\rho(\theta^*)H) = O(\sigma^4)$. In other words, even by studying $E(\theta^*)$ we can adequately predict the behavior of true optimal energy $\delta E(\theta^* + \delta\theta^*)$. For detailed calculations, please refer to appendix C. Indeed, having trained with this type of noise we observe that δE was reduced by no more than 10 – 15% on figures 2 and 3. Finally, since δE can only be reduced by updating the optimal parameters, the established linear behaviour remains a valid upper bounds on energy perturbation.

ACKNOWLEDGEMENT

D.R., E.C., S.A., E.P., D.V. acknowledge support from the research project, Leading Research Center on Quantum Computing (agreement No. 014/20).

-
- [1] John Preskill. Quantum computing in the nisq era and beyond. *Quantum*, 2:79, 2018.
- [2] Johannes Weidenfeller, Lucia C Valor, Julien Gacon, Caroline Tornow, Luciano Bello, Stefan Woerner, and Daniel J Egger. Scaling of the quantum approximate optimization algorithm on superconducting qubit based hardware. *arXiv preprint arXiv:2202.03459*, 2022.
- [3] Alexander K Ratcliffe, Richard L Taylor, Joseph J Hope, and André RR Carvalho. Scaling trapped ion quantum computers using fast gates and microtraps. *Physical Review Letters*, 120(22):220501, 2018.
- [4] Swathi S Hegde, Jingfu Zhang, and Dieter Suter. Toward the speed limit of high-fidelity two-qubit gates. *Physical Review Letters*, 128(23):230502, 2022.
- [5] Adam R Mills, Charles R Guinn, Michael J Gullans, Anthony J Sigillito, Mayer M Feldman, Erik Nielsen, and Jason R Petta. Two-qubit silicon quantum processor with operation fidelity exceeding 99%. *Science Advances*, 8(14):eabn5130, 2022.
- [6] Abhinav Kandala, Antonio Mezzacapo, Kristan Temme, Maika Takita, Markus Brink, Jerry M Chow, and Jay M Gambetta. Hardware-efficient variational quantum eigensolver for small molecules and quantum magnets. *Nature*, 549(7671):242–246, 2017.
- [7] Daniil Rabinovich, Soumik Adhikary, Ernesto Campos, Vishwanathan Akshay, Evgeny Anikin, Richik Sengupta, Olga Lakhmanskaya, Kirill Lakhmanskiy, and Jacob Biamonte. Ion-native variational ansatz for quantum approximate optimization. *Phys. Rev. A*, 106:032418, Sep 2022.
- [8] Guido Pagano, Aniruddha Bapat, Patrick Becker, Katherine S Collins, Arinjoy De, Paul W Hess, Harvey B Kaplan, Antonis Kyprianidis, Wen Lin Tan, Christopher Baldwin, et al. Quantum approximate optimization of the long-range ising model with a trapped-ion quantum simulator. *Proceedings of the National Academy of Sciences*, 117(41):25396–25401, 2020.
- [9] Jacob Biamonte. Universal variational quantum computation. *Physical Review A*, 103(3):L030401, 2021.
- [10] Marco Cerezo, Andrew Arrasmith, Ryan Babbush, Simon C Benjamin, Suguru Endo, Keisuke Fujii, Jarrod R McClean, Kosuke Mitarai, Xiao Yuan, Lukasz Cincio, et al. Variational quantum algorithms. *Nature Reviews Physics*, 3(9):625–644, 2021.
- [11] Matthew P Harrigan, Kevin J Sung, Matthew Neeley, Kevin J Satzinger, Frank Arute, Kunal Arya, Juan Atalaya, Joseph C Bardin, Rami Barends, Sergio Boixo, et al. Quantum approximate optimization of non-planar graph problems on a planar superconducting processor. *Nature Physics*, 17(3):332–336, 2021.
- [12] Gian Giacomo Guerreschi and Anne Y Matsuura. Qaoa for max-cut requires hundreds of qubits for quantum speed-up. *Scientific reports*, 9(1):1–7, 2019.
- [13] Anastasiia Butko, George Micheliannakis, Samuel Williams, Costin Iancu, David Donofrio, John Shalf, Jonathan Carter, and Irfan Siddiqi. Understanding quantum control processor capabilities and limitations through circuit characterization. In *2020 International Conference on Rebooting Computing (ICRC)*, pages 66–75, 2020.
- [14] E Campos, D Rabinovich, V Akshay, and J Biamonte. Training saturation in layerwise quantum approximate optimisation. (*Letter*) *Physical Review A*, 104:L030401, 2021.
- [15] Kieran Dalton, Christopher K. Long, Yordan S. Yordanov, Charles G. Smith, Crispin H. W. Barnes, Normann Mertig, and David R. M. Arvidsson-Shukur. Variational quantum chemistry requires gate-error probabilities below the fault-tolerance threshold, 2022.
- [16] V. Akshay, H. Philathong, M. E.S. Morales, and J. D. Biamonte. Reachability Deficits in Quantum Approximate Optimization. *Physical Review Letters*, 124(9):090504, Mar 2020.
- [17] Edward Farhi, Jeffrey Goldstone, and Sam Gutmann. A quantum approximate optimization algorithm. *arXiv preprint arXiv:1411.4028*, 2014.
- [18] Vishwanathan Akshay, Daniil Rabinovich, Ernesto Campos, and Jacob Biamonte. Parameter concentrations in quantum approximate optimization. *Physical Review A*, 104(1):L010401, 2021.
- [19] Lov K Grover. A fast quantum mechanical algorithm for database search. In *Proceedings of the twenty-eighth annual ACM symposium on Theory of computing*, pages 212–219, 1996.
- [20] Murphy Yuezhen Niu, Sirui Lu, and Isaac L Chuang. Optimizing qaoa: Success probability and runtime dependence on circuit depth. *arXiv preprint arXiv:1905.12134*, May 2019.
- [21] Seth Lloyd. Quantum approximate optimization is computationally universal. *arXiv preprint arXiv:1812.11075*, 2018.
- [22] Mauro ES Morales, Jacob D Biamonte, and Zoltán Zimborás. On the universality of the quantum approximate optimization algorithm. *Quantum Information Processing*, 19(9):1–26, 2020.
- [23] Leo Zhou, Sheng-Tao Wang, Soonwon Choi, Hannes Pichler, and Mikhail D. Lukin. Quantum approximate optimization algorithm: Performance, mechanism, and implementation on near-term devices. *Phys. Rev. X*, 10:021067, Jun 2020.
- [24] Zhihui Wang, Nicholas C Rubin, Jason M Dominy, and Eleanor G Rieffel. X y mixers: Analytical and numerical results for the quantum alternating operator ansatz. *Physical Review A*, 101(1):012320, 2020.

- [25] Lucas T. Brady, Christopher L. Baldwin, Aniruddha Bapat, Yaroslav Kharkov, and Alexey V. Gorshkov. Optimal Protocols in Quantum Annealing and Quantum Approximate Optimization Algorithm Problems. *Physical Review Letters*, 126(7):070505, Feb 2021.
- [26] Edward Farhi and Aram W Harrow. Quantum supremacy through the quantum approximate optimization algorithm. *arXiv preprint arXiv:1602.07674*, 2016.
- [27] Edward Farhi, Jeffrey Goldstone, Sam Gutmann, and Leo Zhou. The quantum approximate optimization algorithm and the sherrington-kirkpatrick model at infinite size. *arXiv preprint arXiv:1910.08187*, Oct 2019.
- [28] Matteo M. Wauters, Glen B. Mbeng, and Giuseppe E. Santoro. Polynomial scaling of the quantum approximate optimization algorithm for ground-state preparation of the fully connected p -spin ferromagnet in a transverse field. *Phys. Rev. A*, 102:062404, Dec 2020.
- [29] Jahan Claes and Wim van Dam. Instance independence of single layer quantum approximate optimization algorithm on mixed-spin models at infinite size. *arXiv preprint arXiv:2102.12043*, 2021.
- [30] Leo Zhou, Sheng-Tao Wang, Soonwon Choi, Hannes Pichler, and Mikhail D. Lukin. Quantum approximate optimization algorithm: Performance, mechanism, and implementation on near-term devices. *Phys. Rev. X*, 10:021067, Jun 2020.
- [31] Vishwanathan Akshay, H Philathong, E Campos, Daniil Rabinovich, Igor Zacharov, Xiao-Ming Zhang, and J Biamonte. On circuit depth scaling for quantum approximate optimization. *arXiv preprint arXiv:2205.01698*, 2022.
- [32] John Clarke and Frank K Wilhelm. Superconducting quantum bits. *Nature*, 453(7198):1031–1042, 2008.
- [33] Jay M Gambetta, Jerry M Chow, and Matthias Steffen. Building logical qubits in a superconducting quantum computing system. *npj quantum information*, 3(1):1–7, 2017.
- [34] L. V. Gerasimov, R. R. Yusupov, A. D. Moiseevsky, I. Vybornyi, K. S. Tikhonov, S. P. Kulik, S. S. Straupe, C. I. Sukenik, and D. V. Kupriyanov. Coupled dynamics of spin qubits in optical dipole microtraps. 2022.
- [35] M. Morgado and S. Whitlock. Quantum simulation and computing with rydberg-interacting qubits. *AVS Quantum Science*, 3(2):023501, 2021.
- [36] J. Zhang, G. Pagano, P. W. Hess, A. Kyprianidis, P. Becker, H. Kaplan, A. V. Gorshkov, Z.-X. Gong, and C. Monroe. Observation of a many-body dynamical phase transition with a 53-qubit quantum simulator. *Nature*, 551(7682):601–604, 2017.
- [37] Kenneth R Brown, John Chiaverini, Jeremy M Sage, and Hartmut Häffner. Materials challenges for trapped-ion quantum computers. *Nature Reviews Materials*, 6(10):892–905, 2021.
- [38] Philipp Schindler, Daniel Nigg, Thomas Monz, Julio T Barreiro, Esteban Martinez, Shannon X Wang, Stephan Quint, Matthias F Brandl, Volckmar Nebendahl, Christian F Roos, et al. A quantum information processor with trapped ions. *New Journal of Physics*, 15(12):123012, 2013.
- [39] Evan PG Gale, Zain Mehdi, Lachlan M Oberg, Alexander K Ratcliffe, Simon A Haine, and Joseph J Hope. Optimized fast gates for quantum computing with trapped ions. *Physical Review A*, 101(5):052328, 2020.
- [40] Jan Benhelm, Gerhard Kirchmair, Christian F Roos, and Rainer Blatt. Towards fault-tolerant quantum computing with trapped ions. *Nature Physics*, 4(6):463–466, 2008.
- [41] Christopher R Monroe and David J Wineland. Quantum computing with ions. *Scientific American*, 299(2):64–71, 2008.
- [42] Laird Nicholas Egan. *Scaling Quantum Computers with Long Chains of Trapped Ions*. PhD thesis, University of Maryland, College Park, 2021.
- [43] A V Uvarov and J D Biamonte. On barren plateaus and cost function locality in variational quantum algorithms. *Journal of Physics A: Mathematical and Theoretical*, 54(24):245301, may 2021.
- [44] Joris Kattemölle and Guido Burkard. Effects of correlated errors on the quantum approximate optimization algorithm, 2022.
- [45] Anders Sørensen and Klaus Mølmer. Quantum computation with ions in thermal motion. *Phys. Rev. Lett.*, 82:1971–1974, Mar 1999.
- [46] Anders Sørensen and Klaus Mølmer. Entanglement and quantum computation with ions in thermal motion. *Phys. Rev. A*, 62:022311, Jul 2000.
- [47] Zhi-Cheng Yang, Armin Rahmani, Alireza Shabani, Hartmut Neven, and Claudio Chamon. Optimizing variational quantum algorithms using ponyryagin’s minimum principle. *Physical Review X*, 7(2):021027, 2017.
- [48] Mohannad M. Ibrahim, Hamed Mohammadbagherpoor, Cynthia Rios, Nicholas T. Bronn, and Gregory T. Byrd. Evaluation of parameterized quantum circuits with cross-resonance pulse-driven entanglers. *IEEE Transactions on Quantum Engineering*, 3:1–13, 2022.

Appendix A: k-SAT, MAX-CUT and unstructured search problems

1. k-SAT

Boolean satisfiability, or SAT, is the problem of determining whether a boolean formula written in conjunctive

normal form (CNF) is satisfiable. It is possible to map any SAT instance via Karp reduction into k -SAT, which are restricted to k literals per clause. In order to approximate solutions to SAT we embed the instance into a Hamiltonian as

$$H_{\text{SAT}} = \sum_j P(j), \quad (\text{A1})$$

where j indexes clauses of an instance, and $P(j)$ is the tensor product of projectors that penalizes bit string assignments that do not satisfy the j -th clause. In this work we focused on the $k = 3$ case.

2. MAX-CUT

Given a graph (V, E) , MAX-CUT is a problem of identifying the maximal cut of the graph, i.e. finding a graph bipartition with maximal number of edges between two components. Any instance of MAX-CUT problem can be encoded as an $n = |V|$ qubit problem Hamiltonian

$$H = \sum_{(i,j) \in E} Z_i Z_j, \quad (\text{A2})$$

whose ground state encodes the solution to the problem: bit string $|z_1 z_2, \dots, z_n\rangle$ corresponds to the partition where i -th vertex belongs to the $z_i = 0, 1$ component.

3. Unstructured search

Consider an unstructured database S indexed by $j \in \{0, 1\}^{\times n}$. Let $f : \{0, 1\}^{\times n} \rightarrow \{0, 1\}$ be a Boolean function (a.k.a. black box) such that:

$$f(j) = \begin{cases} 1 & \text{iff } j = t \\ 0 & \text{otherwise.} \end{cases} \quad (\text{A3})$$

The task is to find $t \in \{0, 1\}^{\times n}$. The corresponding problem Hamiltonian for QAOA is

$$H_t = \mathbb{1} - |t\rangle\langle t|, \quad (\text{A4})$$

thus the expected value is given by

$$\langle H \rangle = 1 - |\langle t | \psi_p(\boldsymbol{\gamma}, \boldsymbol{\beta}) \rangle|^2. \quad (\text{A5})$$

QAOA performance for unstructured search is not sensitive to the particular target state $|t\rangle$ in the computational basis. For any target state $|t\rangle$ representing a binary string, there is a $U = U^\dagger$ composed of X and $\mathbb{1}$ operators such that $U |0\rangle^{\otimes n} = |t\rangle$. The overlap of an arbitrary state prepared by a QAOA sequence with $|t\rangle$ is then:

$$\begin{aligned} \langle t | \psi_p(\boldsymbol{\gamma}, \boldsymbol{\beta}) \rangle &= \langle t | \prod_{k=1}^p e^{-i\beta_k \mathcal{H}_x} e^{-i\gamma_k |t\rangle\langle t|} |+\rangle^{\otimes n} \\ &= \langle 0 |^{\otimes n} U \prod_{k=1}^p e^{-i\beta_k \mathcal{H}_x} e^{-i\gamma_k U(|0\rangle\langle 0|)^{\otimes n} U} |+\rangle^{\otimes n} \\ &= \langle 0 |^{\otimes n} U \prod_{k=1}^p e^{-i\beta_k \mathcal{H}_x} U e^{-i\gamma_k (|0\rangle\langle 0|)^{\otimes n}} U |+\rangle^{\otimes n} \\ &= \langle 0 |^{\otimes n} \prod_{k=1}^p e^{-i\beta_k \mathcal{H}_x} e^{-i\gamma_k (|0\rangle\langle 0|)^{\otimes n}} |+\rangle^{\otimes n}, \end{aligned}$$

which is independent on t .

Appendix B: QAOA for MAX-CUT and unstructured search

1. MAX-CUT

Here we show results of perturbing QAOA circuits, optimized to solve instances of MAX-CUT. We follow the same procedure explained in the main text. We consider 100 randomly generated graphs of $n = 6, 8, 10$ vertices; these graphs were generated by adding edges between every pair of vertices with probability $1/2$. The instances were minimized with circuits of depth 10, 13 and 15, respectively, which guaranteed at least 85% overlap with the ground states. The energies of perturbed circuits are illustrated in Fig. 7. Similar to the results of Section IV our linear prediction holds up to $q\sigma^2 \gtrsim 1$.

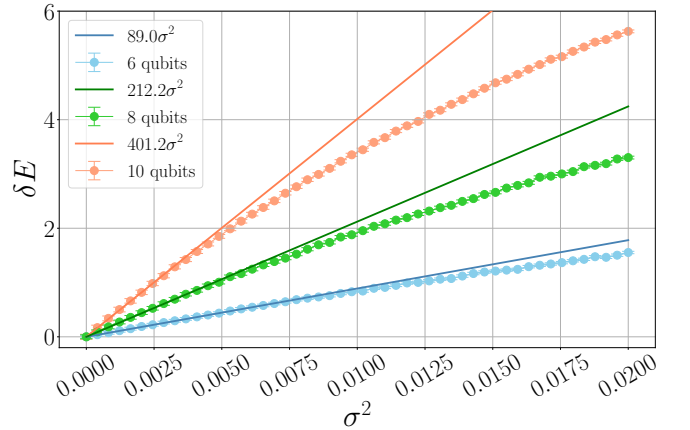


FIG. 7. Average energy shift of 100 instances of of MAX-CUT on 6, 8 and 10 qubits obtained from perturbed optimal circuits of depth 10, 13 and 15, respectively. The instances were designed to approximately have graph density 0.5. Error bars depict standard errors. Polynomial fits of data indicate $\delta E \propto \sigma^2$ up to $q\sigma^2 \gtrsim 1$.

2. Unstructured search

Here we show results of perturbing QAOA circuits, optimized to solve the unstructured search problem. Opposite to the main text, here we consider perturbations introduced to every QAOA layer, without decomposition into gates of the form (7). This corresponds to multiple gates receiving the same perturbation in the settings presented in Section IV. Energy increases of the perturbed optimized circuits are illustrated in Fig. 8. Despite a different setting where problem Hamiltonian propagator is not decomposed into gates of form (7) the energy perturbation still scales linearly with σ^2 at least in the range of small σ , which demonstrates that our result applies even to circuits of a more general type.

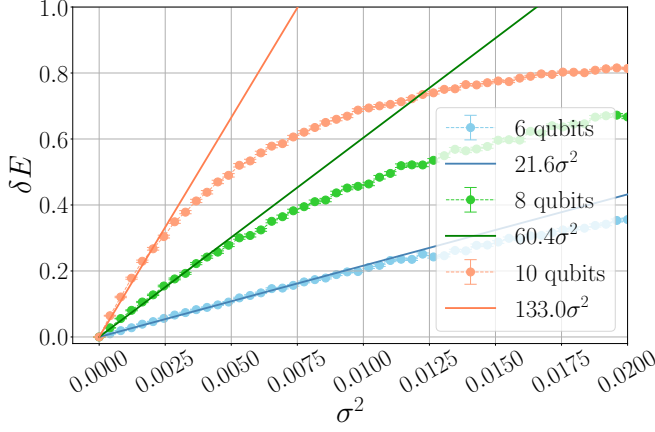


FIG. 8. Average energy for the problem of unstructured search obtained by the perturbation of γ^* , β^* by δ uniformly sampled from the range $(-\sigma, \sigma)$. Error bars depict standard errors. Polynomial fits of data points of 6, 8 and 10 qubits in the ranges $\sigma \in [0, 0.1]$, $[0, 0.07]$, $[0, 0.05]$, respectively confirm that $\delta E \propto \sigma^2$.

Appendix C: Shift of optimal parameters in the presence of noise

Let us use expressions (10) and (11) to estimate change in the energy if one accounts for shift of optimal parameters $\theta^* \rightarrow \theta^* + \delta\theta^*$ in the presence of noise:

$$\begin{aligned} \text{Tr}(\rho(\theta^* + \delta\theta^*)H) &= \\ & (1 - \sum_{k=1}^q a_k) \langle \psi(\theta^* + \delta\theta^*) | H | \psi(\theta^* + \delta\theta^*) \rangle \\ & + \sum_{k=1}^q a_k \langle \psi_k(\theta^* + \delta\theta^*) | H | \psi_k(\theta^* + \delta\theta^*) \rangle + o(\sigma_k^2) \end{aligned} \quad (\text{C1})$$

We introduce gradients of the noisy terms

$$\mathbf{B}^k = \frac{\partial}{\partial \theta} \langle \psi_k(\theta) | H | \psi_k(\theta) \rangle |_{\theta=\theta^*}, \quad (\text{C2})$$

and Hessian \mathbf{H} of the energy at noiseless optimum,

$$\mathbf{H}_{ij} = \frac{\partial^2}{\partial \theta_i \partial \theta_j} \langle \psi(\theta) | H | \psi(\theta) \rangle |_{\theta=\theta^*}. \quad (\text{C3})$$

Notice that gradients of the noiseless function $\langle \psi(\theta) | H | \psi(\theta) \rangle$ vanish at optimum. Then,

$$\begin{aligned} \text{Tr}(\rho(\theta^* + \delta\theta^*)H) &\approx (1 - \sum_{k=1}^q a_k) E^* + \frac{1}{2} (\delta\theta^*)^T \mathbf{H} \delta\theta^* \\ & + \sum_{k=1}^q a_k [\langle \psi_k(\theta^*) | H | \psi_k(\theta^*) \rangle + (\delta\theta^*)^T \mathbf{B}^k]. \end{aligned} \quad (\text{C4})$$

Minimizing it with respect to $\delta\theta^*$ one gets

$$\delta\theta^* = - \sum_{k=1}^q a_k \mathbf{H}^{-1} \mathbf{B}^k. \quad (\text{C5})$$

Thus, if we account for the change of optimal parameters in the presence of noise, the energy shifts by

$$\begin{aligned} \text{Tr}(\rho(\theta^* + \delta\theta^*)H) - \text{Tr}(\rho(\theta^*)H) &\approx \\ & (\delta\theta^*)^T \mathbf{H} \delta\theta^* + \sum_{k=1}^q a_k (\delta\theta^*)^T \mathbf{B}^k = O(\sigma^4). \end{aligned} \quad (\text{C6})$$